OPEN

Citation: Cell Death and Disease (2013) 4, e897; doi:10.1038/cddis.2013.423

www.nature.com/cddis

Irradiation to the young mouse brain impaired white matter growth more in females than in males

K Roughton[1], M Boström[1], M Kalm[1] and K Blomgren*[,1,2,3]

Modern therapy cures 80% of all children with brains tumors, but may also cause long-lasting side effects, so called late effects. Radiotherapy is particularly prone to cause severe late effects, such as intellectual impairment. The extent and nature of the resulting cognitive deficits may be influenced by age, treatment and gender, where girls suffer more severe late effects than boys. The reason for this difference between boys and girls is unknown, but very few experimental studies have addressed this issue. Our aim was to investigate the effects of ionizing radiation on the corpus callosum (CC) in both male and female mice. We found that a single dose of 8 Gray (Gy) to the brains of postnatal day 14 mice induced apoptosis in the CC and reduced the number of proliferating cells by one third, as judged by the number of phospho-histone H3 positive cells 6 h after irradiation (IR). BrdU incorporation was reduced (62% and 42% lower in females and males, respectively) and the number of oligodendrocytes (Olig2$^+$ cells) was lower (43% and 21% fewer in females and males, respectively) 4 months after IR, so the lack of developing and differentiated cells was more pronounced in females. The number of microglia was unchanged in females but increased in males at this late time point. The density of microvessel profiles was unchanged by IR. This single, moderate dose of 8 Gy impaired the brain growth to some extent (8.1% and 0.4% lower brain/body weight ratio in females and males, respectively) but the CC growth was even more impaired (31% and 19% smaller in females and males, respectively) 4 months after IR compared with non-irradiated mice. In conclusion, this is the first study to our knowledge demonstrating that IR to the young rodent brain affects white matter development more in females than in males.

Cell Death and Disease (2013) **4,** e897; doi:10.1038/cddis.2013.423; published online 31 October 2013
Subject Category: Neuroscience

Brain tumors are the most common solid tumors in pediatric patients.[1,2] Childhood cancer survival has increased over the last decades and today more than 75% of pediatric brain tumor patients survive more than 5 years.[3] This increased survival is due to improved and more personalized surgery, chemotherapy and radiotherapy.[4,5] However, cranial radiotherapy (CRT) during childhood can cause adverse side effects such as hormonal imbalances, growth retardation and persistent impaired learning and memory function.[6] Female gender and young age at the time of radiotherapy are associated with a greater risk of cognitive decline, including processing speed.[7–9] Further, CRT is associated with the loss of white matter both in the human and rodent brain.[10,11] CRT has been shown to cause hypomyelination in children treated for malignant brain tumors.[12] CRT affects many areas and cell types in the CNS but the underlying pathogenesis is not well understood. It is believed that the negative cognitive effects seen after CRT are due to, at least partly, reduced hippocampal neurogenesis.[13–15] Neurocognitive deficits after CRT have also been linked to the loss of white matter.[16] Reddick *et al.*[17] showed that white matter volume decreased in patients with medulloblastoma treated with craniospinal irradiation (IR). Moreover, they showed that younger age at the time of treatment had a significant negative effect on the white matter volume.[17] The corpus callosum (CC), the largest white matter commissure, is affected in children subjected to CRT, with the greatest effects observed in the most posterior subregions (isthmus and splenium).[18] These regions grow from late gestational age until adulthood, with the highest growth rates during early childhood.[19–21] Myelination was shown to be impaired in immature and juvenile rats subjected to cranial IR, but the effect was much more pronounced in the immature rat brain.[22]

The vasculature has an important role in the regulation of survival and proliferation of surrounding stem cells in the brain.[23] In addition, oligodendrocytes have a close relationship with the vasculature in the brain and are involved in the angiogenic response seen after white matter injury,[24] suggesting the presence of an oligovascular niche, analogous to the neurovascular niche promoting recovery in the gray matter after injury. In a previous study, we proposed that the hippocampal vasculature adjusts to the needs of the

[1]Center for Brain Repair and Rehabilitation, Institute of Neuroscience and Physiology, University of Gothenburg, Gothenburg, Sweden; [2]Department of Pediatrics, University of Gothenburg, Queen Silvia Children's Hospital, Gothenburg, Sweden and [3]Karolinska Institutet, Department of Women's and Children's Health, Karolinska University Hospital, Stockholm, Sweden
*Corresponding author: K Blomgren, Karolinska Institutet, Department of Women's and Children's Health, Karolinska University Hospital, Q2:07, SE 171 76, Stockholm, Sweden. Tel: +46 8 517 771 83; Fax: +46 8 517 717 74; E-mail: klas.blomgren@ki.se
Keywords: Sex; cranial radiotherapy; CD31; S100; active caspase-3; Iba-1
Abbreviations: $^+$, positive; BrdU, bromodeoxyuridine; CC, corpus callosum; CD31, Cluster of Differentiation 31; CRT, cranial radiotherapy; ELISA, enzyme-linked immunosorbent assay; Gy, Gray; Iba-1, ionized calcium-binding adapter molecule 1; IHC, immunohistochemistry; IR, irradiation; MBP, myelin basic protein; P, postnatal day; PHH3, phospho-histone H3; Olig2, oligodendrocyte lineage transcription factor 2; S100, S100 calcium-binding protein
Received 09.8.13; revised 24.9.13; accepted 25.9.13; Edited by A Verkhratsky

surrounding neural and glial tissue after IR.[25] In a study by Wakisaki *et al.*,[26] microscopic necrotic lesions were found to be widely dispersed in the white matter located in the forebrain of adult monkeys exposed to 60 Gray (Gy) fractionated cranial IR. In addition, the number of lesions increased with time after IR, and was followed by both patches of telangiectasia and focal vascular endothelial hyperplasia.

As memory and learning are closely related to hippocampal neurogenesis, experimental studies of IR-induced cognitive decline tend to focus mainly on this process, whereas the effects on other brain regions are often overlooked. Most studies use male animals and do not take sex into consideration. However, previous studies have shown sex-dependent differences in the hippocampus in response to cranial IR.[27,28] In the current study, we characterized the effects of IR on the white matter in both male and female mice, demonstrating more pronounced negative effects of IR in females.

Results

Experimental design. An overview of the experimental design is shown in Figure 1.

Growth of the CC after cranial IR. The volume of the CC (outlined in Figure 2a) was measured 6 h and 4 months post IR. We did not see any differences in volume at the early time point, neither after IR nor between the sexes (Figure 2b). Four months after IR, however, growth retardation was observed in the CC and females displayed a more pronounced growth retardation compared with males (19.3% in the male and 30.6% smaller in the female CC, Figure 2b, interaction, $P = 0.038$).

Proliferation and cell death in the CC after IR

Phospho-histone H3: Proliferating cells are particularly susceptible to IR.[27,29,30] Proliferation was measured by quantification of phospho-histone H3 positive ($H3^+$) ($PHH3^+$) cells in the CC 6 h post IR (Figure 3a). $PHH3^+$ cells were evenly distributed throughout the CC. After IR, there was a reduction in both males and females (Figure 3b, $P = 0.001$), no sex differences were observed at this time point after IR.

Active caspase-3: Apoptotic cells, as judged by immunostaining for active caspase-3, were also evenly distributed throughout the CC (Figure 3c). Quantification of the number of apoptotic cells 6 h post IR showed that IR induced caspase-3-dependent cell death in this area (Figure 3d, $P < 0.001$), and the number of dying cells was approximately in the same range as the loss of proliferating cells (Figure 3b). There was no difference between the sexes at this time point.

Brain weight: The whole brain (as defined in Materials and Methods) was weighed 4 months post IR and normalized to body weight (Figure 4a). We observed a difference between sexes in the response to IR, where females showed a greater IR-induced brain growth retardation compared with males (0.4% decrease in males and 8.1% decrease in females, Figure 4b, interaction, $P = 0.016$). Non-IR females displayed a 30.2% higher brain per body weight ratio compared with non-IR males.

Myelin basic protein: Myelin basic protein (MBP) was measured in both hemispheres 4 months post IR. We did not observe any IR-induced reduction at this time point, but we did observe a difference between the sexes, where females had a larger amount of this protein compared with males (Figure 4c, $P < 0.001$).

Survival of cells in the CC in the adult mouse brain

Bromodeoxyuridine: Bromodeoxyuridine (BrdU) labeling 3 months after IR followed by quantification of the number of labeled, surviving cells in the CC 4 weeks later (4 months post IR, Figure 5a), revealed a lower number of cells in the CC in irradiated males and females. An interaction was detected between sex and treatment, showing that females were more susceptible to IR, as judged by a greater reduction in the number of labeled cells in the CC (41.8% loss in males and 62.2% loss in females 4 months post IR, Figure 5b, $P = 0.033$).

Oligodendrocytes in the CC: Oligodendrocyte lineage transcription factor 2 (Olig2) was used as a marker of oligodendrocytes in the CC (Figure 5c). A difference after IR was observed in the Olig2 counts, where non-IR animals showed higher numbers of oligodendrocytes compared with IR animals ($P < 0.001$) and we detected an interaction between sex and treatment, where irradiated females displayed a greater reduction in the number of $Olig2^+$ cells compared with males (21.1% decrease in males and 43.0% decrease in females, Figure 5d, $P = 0.004$).

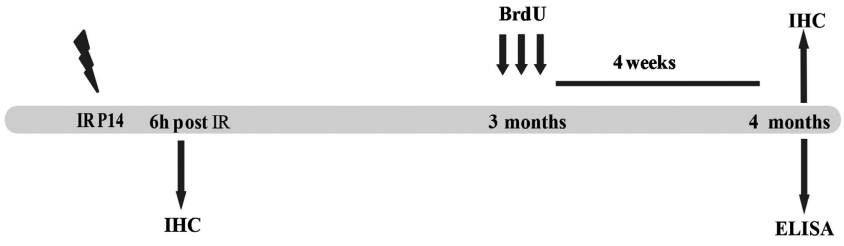

Figure 1 An overview of the timeline of the study. At P14, the animals were subjected to 8 Gy of IR. One group of animals were killed 6 h post IR and used for IHC. The second group were given three doses of BrdU at the age of 3 months and then killed 4 weeks later (4 months old) and used for IHC. In the third group, the brains were collected for ELISA at the same time point as the second group (4 months old)

Astrocytes in the CC: S100 calcium-binding protein (S100) was used as a marker for astrocytes in the CC and was quantified 4 months post IR (Figure 5e). There was a difference after IR in the total number of astrocytes in the CC, where IR animals showed a lower number of these cells (Figure 5f, $P=0.012$).

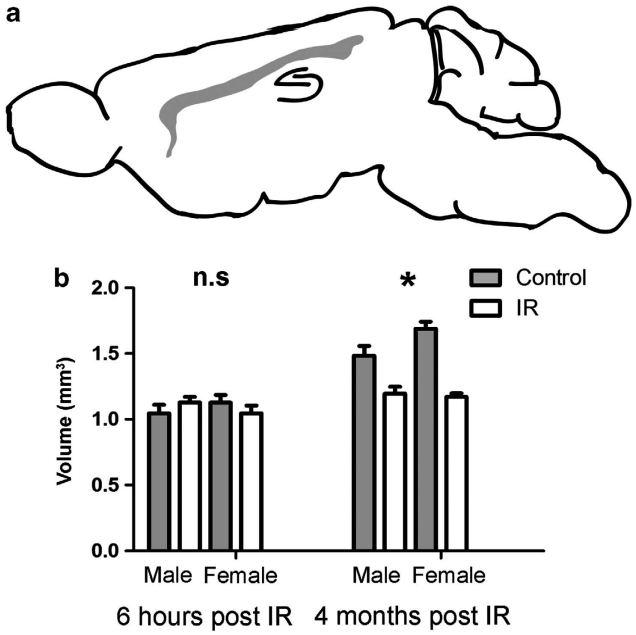

Figure 2 (**a**) Shows a schematic illustration of a sagittal rodent brain with the CC outlined in gray. (**b**) Shows the volume of the CC at 6 h post IR (to the left) and 4 months post IR (to the right). All data shown as mean ± S.E.M. $^{*}P<0.05$ for interaction between treatment and sex

Microglia in the CC: Ionized calcium-binding adapter molecule 1 (Iba-1) was used as a marker for microglia. The number of microglia was quantified 4 months post IR (Figure 5g). There was a difference in the density of microglia in the CC, such that IR males showed an increased density, whereas IR females showed no difference in the density of microglia compared with control animals (45.5% increase in males and 3.4% in females, Figure 5h, $P=0.031$ for treatment and $P=0.030$ for sex).

Vascular status of the CC after IR. The vasculature was visualized with the help of an antibody against Cluster of Differentiation 31 (CD31, Figures 6a and b). A difference after IR was observed for both total vessel surface area ($P<0.001$) (Figure 6c and Table 1) and total number of vessels ($P<0.001$) (Table 1), where irradiated animals had lower numbers compared with control animals. However, no difference was observed between irradiated and control animals in the densities for the same parameters (Table 1). No difference between the sexes was observed, neither for total numbers nor for density values.

Vessel characteristics and shape: We investigated the structural vessel characteristics listed in Materials and Methods and observed a sex difference in one out of four parameters (Table 1). The vessels of female mice had an increased breadth ($P=0.018$) compared with male mice.

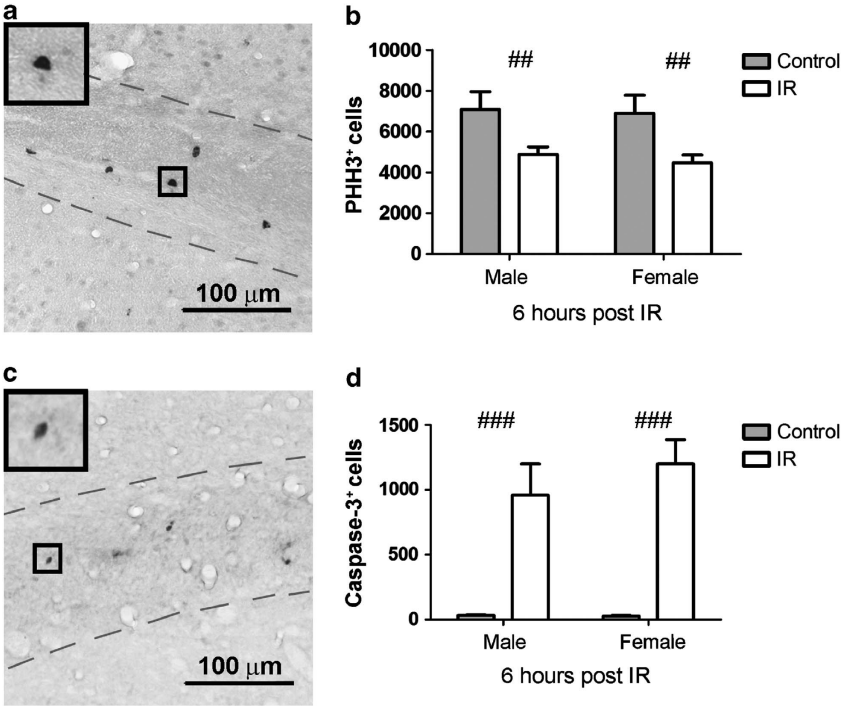

Figure 3 (**a**) Shows a representative microphotograph of PHH3^{+} cells in the CC from control mouse brain. (**b**) Shows a quantification of PHH3^{+} cells 6 h post IR. (**c**) Shows a representative microphotograph of active caspase-3^{+} cells in the CC in IR mouse brain. (**d**) Shows a quantification of active caspase-3^{+} cells at 6 h post IR. All data shown as mean ± S.E.M. $^{\#\#}P<0.01$, $^{\#\#\#}P<0.001$ for treatment

a		Body weight (g)		Brain weight (g)	
		Mean	± SEM	Mean	± SEM
Males	Control	28.9	0.309	0.387	0.004
	IR	27.7	0.367	0.370	0.004
Females	Control	21.5	0.343	0.412	0.005
	IR	21.0	0.483	0.369	0.005

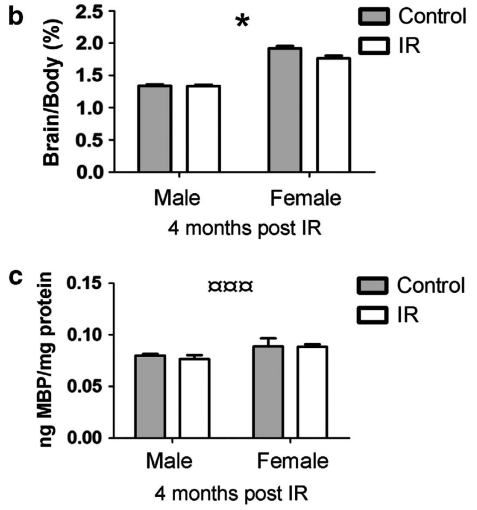

Figure 4 (**a**) Shows the body and the brain weight 4 months post IR. (**b**) Shows the brain weight per body weight ratio (%) 4 months post IR. (**c**) Shows the MBP in cortex tissue 4 months post IR. All data shown as mean ± S.E.M. $^{*}P<0.05$ for interaction between sex and treatment, $^{¤¤¤}P<0.001$ for sex

In addition, there was a tendency toward an increased vessel perimeter in female mice ($P=0.054$). No difference was observed in the remaining factors (vessel length and mean radius). No difference was observed for any of the structural vessel parameters after IR.

Furthermore, we investigated the shape factor of the analyzed vessels, where a number of 0 represents a completely circular vessel and a number of 1 represents a completely flattened vessel. There were no differences, neither after IR nor between the sexes, and the average shape factor was below 0.5 in all groups.

Discussion

The aim of the present study was to explore the cellular response in the CC after IR to the young mouse brain. White matter damage caused by IR has been studied before,[22,31,32] but to the best of our knowledge, differences between the sexes have not been studied. This is important, as different effects after CRT have been observed in patients, such that girls suffer more severe late effects compared with boys.[7,33,34] White matter integrity has been shown to be important for cognitive performance,[35] but very few studies have taken this into account when investigating the effects of IR in animal models.

The number of callosal fibers (~200 million) is already fixed around birth, but structural changes of the CC continue to occur during postnatal development due to fiber myelination, redirection and pruning.[19] The growth rate of the CC is highest during the first years of life, but it continues to grow during childhood and adolescence, and the difference in growth rates between males and females is most pronounced during adolescence.[20,21] Myelination in the human brain continues during childhood, adolescence and into the third and fourth decades of life in specific brain regions.[36,37] Oligodendrocytes generate myelin sheaths needed to facilitate the conduction of action potentials during neuronal signaling within the CNS.[36,38] Myelination in the rat brain starts at P10, accelerates between P16 and P30 and peaks around P20.[31,39] In addition, the peak of oligodendrogenesis occurs during the second postnatal week in rats, just before the acceleration of myelination.[40] Hence, the time of IR in our study (P14) coincided with high oligodendrocyte proliferation, early growth and rapid myelination of the CC. We irradiated animals on P14, long before they were sexually mature so the estrous cycle should not be a confounding factor in the females. IR to the young brain does not only cause acute injury, but will inevitably interfere with further growth of developing brain structures, including the CC.

There was no difference in the CC volume in the acute phase (6 h post IR), but we observed reduced proliferation ($PHH3^{+}$ cells) in both sexes after IR. Similarly, a 16-fold decrease in proliferating cells in the CC, as measured by BrdU incorporation, was shown one day after 25 Gy to young adult female rats (3 months).[41] Consistent with reduced proliferation, we observed increased active caspase-3-dependent cell death in the CC of irradiated males and females. Apoptosis in the CC has previously been reported after IR to the young adult female (3 months) rat brain, with a peak 6 h post IR, the same time point after IR as in the current study.[42] Earlier studies have shown oligodendrocyte cell death in the CC 24 h post IR in the rat brain, with a peak 8 h post IR.[43] The death of proliferating progenitors in the CC likely contributes to the observed growth retardation of the CC 4 months post IR. At this time point, irradiated females displayed a greater growth retardation in the CC compared with their male counterparts. Similar growth retardation has previously been observed in the mouse hippocampus exposed to the same dose of IR (8 Gy), at the same age (P14), as in the current study.[27] The differential effect in CC volume between the sexes after IR was also reflected in the brain/body weight ratio, where irradiated females proved to be more radiosensitive, displaying an 8.1% lower ratio in IR females compared with 0.4% in IR males, that is, a 20-fold greater effect of IR in females. We did not observe any IR-induced difference in MBP, neither in males nor in females. The lack of IR-induced changes in MBP is consistent with another study reporting unchanged levels of MBP up to 9 months of age in female rats. However, 15 months post IR a drastic demyelination was observed (46% decrease compared with controls), albeit after a considerably higher dose (25 Gy).[41] In the current study, the IR-induced effects were examined up to 4 months post IR, hence late demyelination in the aged brain caused by IR had probably not yet occurred.

Both BrdU and Olig2 quantifications showed a similar pattern in the response to IR, indicating that pre-oligodendrocytes presumably are the main victims of IR in the developing brain, resulting in a smaller number of cells that can develop into oligodendrocytes. Fully differentiated

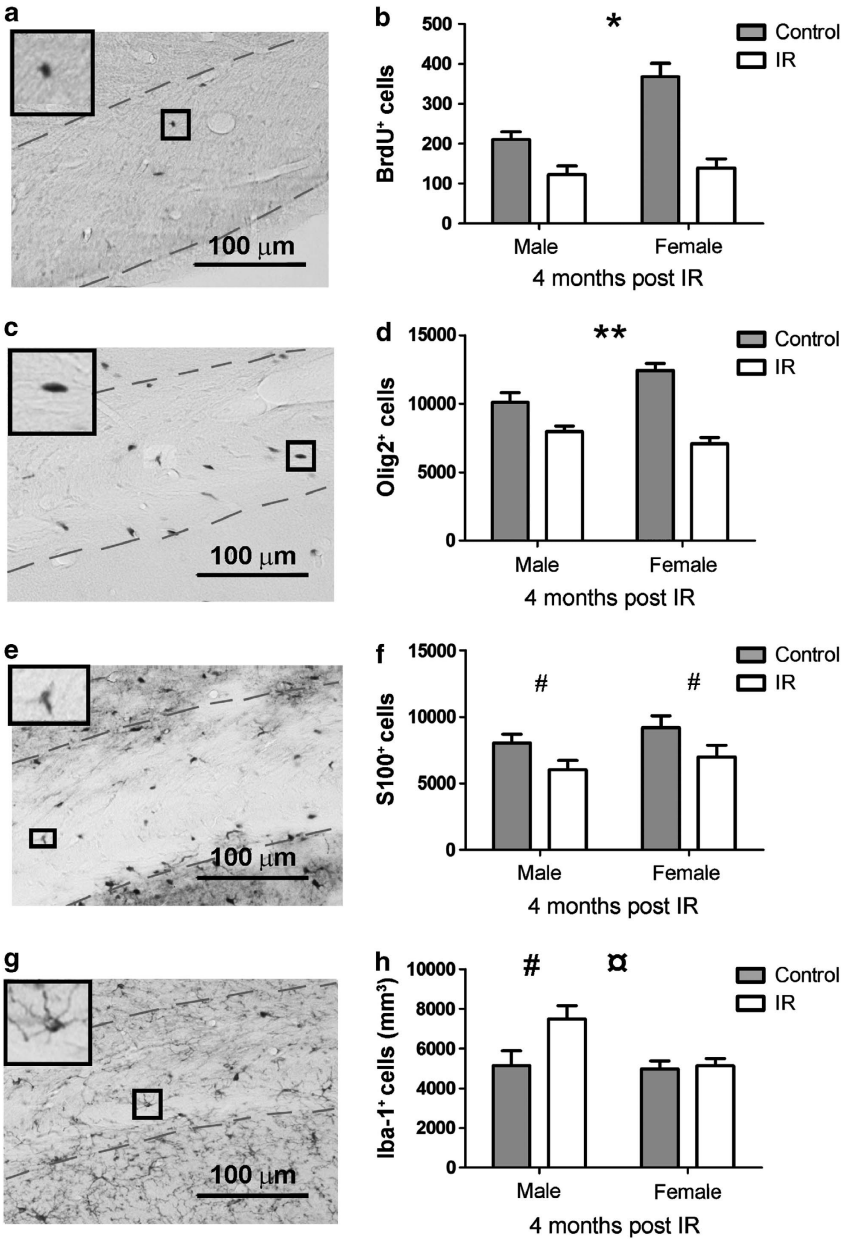

Figure 5 The panels to the left show representative photographs of the different stainings ((**a**) BrdU$^+$ cells, (**c**) Olig2$^+$ cells, (**e**) S100$^+$ cells and (**g**) Iba-1$^+$ cells). The right panels show the quantifications of the different cell types ((**b**) BrdU$^+$ cells, (**d**) Olig2$^+$ cells, (**f**) S100$^+$ cells and (**h**) Iba-1$^+$ cells at 4 months post IR). All data shown as mean ± S.E.M. $^*P<0.05$, $^{**}P<0.01$ for interaction between sex and treatment, $^{¤}P<0.05$ for sex, $^{\#}P<0.05$ for treatment

Table 1 The analyzed vessel parameters are shown in the table below

	Male C	Male IR	Female C	Female IR	(*P*-value)
	n = 10	*n* = 8	*n* = 11	*n* = 11	
Total vessel surface area (mm^2)	0.35 (±0.041)	0.26 (±0.016)	0.41 (±0.015)	0.27 (±0.010)	### (2.5E − 05)
Density, vessel area (%)	6.7% (±0.73)	7.0% (±0.47)	7.3% (±0.28)	7.1% (±0.29)	n.s.
Total numbers of vessels	638 997 (±62 901)	506 719 (±40 985)	695 738 (±26 843)	448 428 (±12 452)	### (2.4E − 05)
Density of vessels (vessels/mm^3)	406 911 (±38 582)	432 468 (±18 698)	399 811 (±8919)	383 514 (±9228)	n.s.
Length (μm)	26.5 (±0.84)	25.9 (±1.70)	27.7 (±0.89)	27.5 (±0.58)	n.s
Breadth (μm)	12.6 (±0.34)	12.4 (±0.63)	13.3 (±0.27)	13.4 (±0.20)	¤¤ (0.018)
Perimeter (μm)	86.4 (±3.05)	83.7 (±5.83)	92.6 (±3.23)	91.6 (±2.25)	n.s
Mean radius (μm)	7.7 (±0.24)	7.6 (±0.49)	8.1 (±0.25)	8.1 (±0.17)	n.s
Shape factor (number between 0 and 1)	0.32 (±0.006)	0.34 (±0.008)	0.34 (±0.007)	0.35 (±0.009)	n.s

C, control; IR, irradiation
All data are shown as mean ± SEM. $^{¤¤}P<0.01$ for sex, $^{\#\#\#}P<0.001$ for treatment

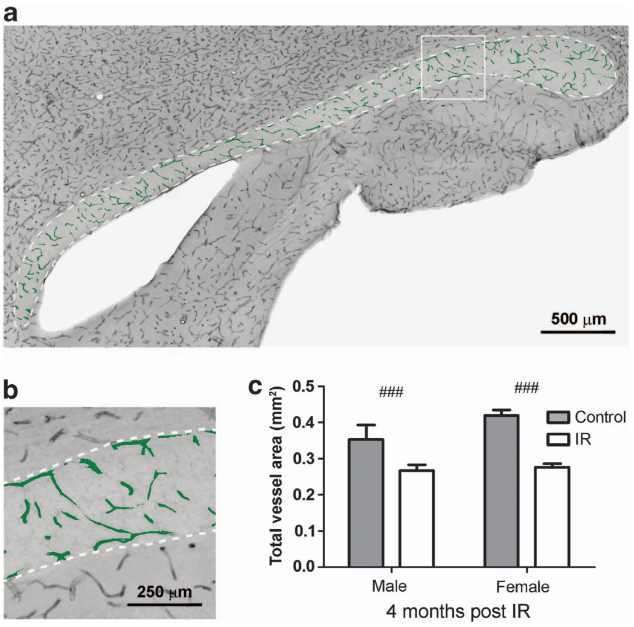

Figure 6 (**a**) Shows a representative microphotograph of the CD31 staining in the CC where the vessels analyzed with metamorph are colored in green. (**b**) Shows a magnification of the analyzed vessels. (**c**) Shows a quantification of the total vessel surface area in the CC 4 months post IR. All data shown as mean ± S.E.M. $^{###}P < 0.001$ for treatment

oligodendrocytes are sensitive to oxidative stress, due to their high metabolic rate.[44] IR causes oxidative stress,[45–47] and this might be one explanation to the observed loss of Olig2$^+$ cells after IR, in addition to the direct loss of pre-oligodendrocytes due to IR-induced DNA damage. IR-induced injury to fully differentiated oligodendrocytes might also contribute to later-occurring loss of white matter in the aging brain, both because of delayed oligodendrocyte death and because the irradiated oligodendrocytes appear to be functionally impaired.[48] We found that females were more susceptible to IR-induced loss of Olig2$^+$ and BrdU$^+$ cells, which could, at least partly, be explained by their higher numbers of BrdU$^+$ cells in the CC compared with non-IR males. Similar results were reported in adult female mice (9 months old) having BrdU incorporation rates twice as high as in males.[49] It is important to bear in mind that pre-oligodendrocytes in rats appear to be more susceptible to IR compared with mice, at least in the spinal cord,[48] and therefore studies performed in different species, as well as strains and sexes, may yield different results. We observed that irradiated females showed a more pronounced loss of BrdU$^+$ and Olig2$^+$ cells, ending up on the same level as irradiated males. This is analogous to the higher hippocampal neurogenesis in female mice dropping to the same level as in irradiated males.[27] Together, these effects likely explain some of the cognitive deficits seen in both rodents and humans after IR, where females/girls have been shown to be more susceptible to IR.[7,27,28,34] We have earlier characterized the IR-induced cognitive impairment in mice of the same age.[50] We have also demonstrated sex-dependent cognitive differences, such that females were shown to be more susceptible to cranial IR than males and females were more anxious.[27]

After brain injury, such as, for example, stroke, the so called neurovascular niche is involved in the neuronal regeneration during functional recovery of cortical gray matter.[51] In another study focused on focal white matter brain injury, it was revealed that oligodendrocytes produced matrix metalloproteinase-9 which facilitated the angiogenic response after injury. In addition, CD31$^+$ microvessels were observed in close proximity to MBP$^+$ oligodendrocytes in the injured demyelinated areas. They therefore suggested that the white matter harbors an oligovascular niche, that similar to the neurovascular niche in gray matter may have a crucial role in the vascular plasticity during brain recovery.[24] It has previously been proposed that white matter in the brain is more vulnerable to IR than gray matter because white matter harbors fewer capillaries.[52] In the current study, we show that irradiated animals had fewer vessels and a smaller total vessel surface area in the CC compared with controls, consistent with our findings in the irradiated mouse hippocampus.[25] However, as in the previous study we did not find any IR-induced difference in the vessel density, suggesting that the vasculature adjusts to the growth-impaired CC, at least morphologically. This argues against white matter vasculature being more susceptible to IR compared with gray matter. It is important to note that the investigation of the vasculature in this study was solely focused on vessel morphology. Other factors, such as vascular permeability and molecular changes could have an important impact on the integrity and function of the CC but were beyond the scope of this study.[53]

In conclusion, this is the first study to our knowledge demonstrating that IR to the young rodent brain affected white matter development more in females than in males. This is consistent with earlier findings from our group and clinical studies showing that girls suffer more severe late effects after CRT than boys. It is not known why girls are more sensitive to CRT than boys, but the current study demonstrates the usefulness of this mouse model in the search for the underlying mechanisms.

Materials and Methods

Animals. Male and female C57BL/6J mice were used (Charles River Laboratories, Sulzfeld, Germany). The animals were kept on a 12-h light cycle. Food and water were provided *ad libitum.* All experiments were approved by the Gothenburg committee of the Swedish Animal Welfare Agency (46-2007, 30-2008, 423-2008 and 326-2009).

IR procedure. For the IR procedure, a linear accelerator (Varian Clinac 600 CD; Radiation Oncology Systems LLC, San Diego, CA, USA) with a 4 MV nominal photon energy and a dose rate of 2.3 Gy/min was used. Male and female littermates were anesthetized on postnatal day 14 with an intraperitoneal tribromoethanol injection (50 mg/kg) and then placed in prone position on a polystyrene bed. The head was covered with a 1 cm tissue equivalent material to obtain an even IR dose throughout the underlying tissue. The whole brain was irradiated with an IR field of 2 × 2 cm and the source to skin distance was ~99.5 cm. An absorbed dose of 8 Gy was administered. A single dose of 8 Gy is equivalent to 18 Gy delivered in 2 Gy fractions, according to the linear quadratic formula and an alpha/beta ratio of 3 for late effects in the normal brain tissue.[54] Control animals were anesthetized but not subjected to IR. After IR, the pups were returned to their dams. Animals were euthanized 6 h post IR (20 males and 20 females) or 4 months post IR (30 males and 30 females for immunohistochemistry (IHC), 30 males and 30 females for enzyme-linked immunosorbent assay, ELISA). The study outline is presented in Figure 1.

BrdU labeling. Animals were given one daily injection of BrdU (50 mg/kg) for 3 consecutive days at the age of 3 months. All BrdU injections were given in the beginning of the active period. Four weeks later the animals were euthanized (4 months post IR).

Immunohistochemistry. Animals were deeply anesthetized with sodium pentobarbital (Pentothal, Electra-box Pharma, Tyresö, Sweden) before being transcardially perfused with a 6% formaldehyde solution buffered with sodium phosphate at pH 7.4 and stabilized with methanol (Histofix; Histolab products AB, Gothenburg, Sweden). The brains were immersion-fixed in Histofix for 24 h after perfusion and then changed to 30% sucrose solution containing 100 mM phosphate buffer, pH 7.5. Before further processing, the brain stem was cut at the base of the cerebellum and then the whole formaldehyde-fixed brain was weighed ($n = 15$). As differences in body weight could be reflected in brain weight, we compensated for this by dividing brain weight with body weight.

The right hemisphere was cut into 25-μm sagittal sections in a series of 12, using a sliding microtome. The sections were stored in a cryoprotection solution, containing 25% ethylene glycol and 25% glycerol, at 4 °C, until staining.

For antigen retrieval, sections to be stained for phospho-histone H3 (PHH3) were treated with 10 mM sodium citrate at 80 °C for 30 min. To block endogenous peroxidases the sections were treated with 0.6% hydrogen peroxide. After rinsing with Tris-buffered saline (TBS, Tris-HCl, 150 mM NaCl, pH 7.5) the sections stained for BrdU were treated with 2 M HCl at 37 °C for 30 min, followed by 10 min in 100 mM borate buffer (pH 8). To block nonspecific binding, the sections were treated with 3% donkey serum in TBS with 0.1% Triton X-100 for 30 min (Jackson Immunoresearch Laboratories Inc, West Grove, PA, USA). Sections were incubated at 4 °C overnight with primary antibodies against PHH3 (rabbit anti-PHH3, 1:1,000, Millipore/Chemicon, Billerica, MA, USA), BrdU (rat anti-BrdU, 1 : 500, AbD Serotec, Kidlington, UK), Olig2 (goat anti-Olig2, 1 : 1000, R&D Systems, Minneapolis, MN, USA), Iba-1 (rabbit anti-Iba-1, 1 : 1000, Wako Pure Chemical Industries Ltd. Osaka, Japan), active caspase-3 (rabbit anti-active caspase-3, 1 : 250, BD Bioscience Pharmingen, Franklin Lakes, NJ, USA), S100 (rabbit-anti-S100, 1 : 5000, Dako Cytomation, Glostrup, Denmark), CD31 (rat anti-mouse CD31, 1 : 2000, BD Bioscience Pharmigen, Franklin Lakes, NJ, USA) diluted in 3% donkey serum in TBS containing 0.1% Triton X-100. The following day, the sections were rinsed and a biotinylated secondary antibody was added for 1 h at room temperature (20 °C) (donkey anti-rabbit IgG, 1 : 1000, donkey anti-rat, IgG 1 : 1000, or donkey anti-goat IgG, 1 : 1000, IgG, all from Jackson Immunoresearch Laboratories Inc). A biotin–avidin solution was added for 1 h (Vectastain ABC Elite kit, Burlingame, CA, USA) and staining was developed using 3-3′-diaminobenzindine tetrahydrochloride (DAB, Saveen Werner AB, Malmö, Sweden) diluted in TBS containing hydrogen peroxide and nickel chloride to enhance the reaction. All primary antibodies used in this report have been well validated[25,29,55–59] and all antibodies (except anti-active caspase-3, which was validated in Zhu *et al.*)[60] are included in the Neuroscience Information Framework (http://www.neuinfo.org) list of thoroughly characterized antibodies (numbers 310177, 609566, 2157554, 839504, 10013383 and 393571 respectively). Omission of the primary antibodies yielded only very weak nonspecific staining, and the identification of the immunopositive cells was facilitated by their characteristic morphology and location.

Cell counting and volume assessment. BrdU-, PPH3-, Olig2-, active caspase-3-, Iba-1- and S100-positive cells were counted throughout the CC in all sections containing a clearly separated/divided dorsal and ventral hippocampus, using stereological principles (Stereoinvestigator, MicroBrightField, Colchester, VT, USA). The CC area was traced at $\times 10$ magnification with a DIC filter. All immunopositive cells in the CC were counted in every 12th section in the right hemisphere in $\times 40$ magnification, resulting in 5–7 sections per animal ($n_{(6\,\text{h post IR})} = 7$–$9$, $n_{(4\text{ months post IR})} = 9 - 15$). Total volumes were calculated according to the Cavalieri principle, using the following formula: $V = SA \times P \times T$, where V is the total volume, SA is the sum of area measurements, P is the inverse of the sampling fraction and T is the section thickness. The total number of cells was obtained by multiplying the number of counted cells with the sampling fraction.

Enzyme-linked immunosorbent assay. Animals used for ELISA were anesthetized with isoflurane, 4–5% in a mixture of 50% oxygen and air. The brains were quickly dissected out, frozen in isopentane and dry ice and stored at -80°C. The tissue was homogenized by sonication in 1 ml of PBS containing 0.1% Triton X-100, 1% protease inhibitor cocktail (Complete mini, Roche Diagnostics GmbH, Penzberg, Germany) and 5 mM EDTA. Crude cytosolic fractions were produced by centrifuging homogenates at $15\,000 \times g$ for 10 min at 4 °C, subsequently stored at -80 °C. Total protein concentration was measured using a NanoDrop Spectrophotometer (Thermo Scientific, Wilmington, DE, USA). ELISA was used to measure the content of MBP (E90539Mu, Uscn, Life Science Inc, Wuhan, China). The whole cortex, including the CC, from each animal was used and ELISA analyses were performed according to the instructions of the manufacturer ($n = 9$–14 per group).

Vascular morphology analysis. The CC was traced at $\times 10$ magnification using a Leica light microscope. With the help of Stereo Investigator's virtual tissue module, multiple images were acquired and stitched together in order to create one single image of the whole structure. This resulted in high resolution images of the CD31 vessel stain that could be used for vessel morphology analysis.

All vessel morphology analyses where performed using the Metamorph Offline software (Metamorph, Microscopy Automation and Image Analysis Software 2011, Molecular Devices Inc., Sunnyvale, CA, USA). Each image was manually inspected and a threshold was set to define the positive CD31 staining against the background. The measurements were then performed using the integrated morphometry analysis module ($n = 8$–11 per group). All analyses were measured in pixels and later recalculated into μm (1 pixel equal to 0.732 μm or 0,536 μm^2). Objects less than 50 pixels were considered nonspecific/debris and consequently excluded from the analysis. After the analysis, all images were once again inspected to manually exclude possible staining artifacts. In this study, we analyzed the following parameters:

- Total vessel surface area: total area positive for the CD31 staining.
- Total number of vessels: total number of measured objects.
- Length: the length of the longest chord through the vessel.
- Breadth: the caliper width of the vessel, perpendicular to the longest chord.
- Perimeter: the distance around the edge of the vessel.
- Mean radius: the average distance from the centroid of the vessel to all points along its edge.
- Shape factor: a value between 0 and 1 describing how closely the vessel approximates a circle, where a value near 0 indicated a flattened object and a value of 1 indicates a perfect circle. Calculated using the following equation: $4\pi A/P^2$, where P = perimeter and A = area.

Statistical analysis. Data from cell counting, vessel analysis and ELISA were analyzed using two-way ANOVA. Treatment, sex and an interaction between the two were considered as main effects. Statistical analysis was performed using SPSS 21.0 (SPSS, Chicago, IL, USA) and significance was assumed when $P < 0.05$. All data are shown as mean ± S.E.M.

Conflict of Interest

The authors declare no conflict of interest.

Acknowledgements. This work was supported by the Swedish Childhood Cancer Foundation (Barncancerfonden), the Swedish Research Council (Vetenskapsradet), the Swedish Cancer Foundation (Cancerfonden), governmental grants from *Agreement concerning research and education of doctors* (ALF), the Sahlgrenska Academy at the University of Gothenburg, the Sten A Olsson's Foundation, the Frimurare Barnhus Foundation, the Wilhelm and Martina Lundgren Foundation, the Gothenburg Medical Society, the Aina Wallström's and Mary-Ann Sjöblom's Foundation, the Ulla and Rune Amlöv Foundations, AFA Insurance and the Swedish Society of Medicine. We are grateful for the skillful technical assistance of Rita Grandér.

1. Parkin DM, Stiller CA, Draper GJ, Bieber CA. The international incidence of childhood cancer. *Int J Cancer* 1988; **42**: 511–520.
2. Steliarova-Foucher E, Stiller C, Kaatsch P, Berrino F, Coebergh JW, Lacour B *et al.* Geographical patterns and time trends of cancer incidence and survival among children and adolescents in Europe since the 1970s (the ACCISproject): an epidemiological study. *Lancet* 2004; **364**: 2097–2105.

3. Gustafsson G, Kogner P, Heyman M. Childhood Cancer Incidence and Survival in Sweden 1984-2010. *Report from the Swedish Childhood Cancer Registry* 2013; http://www.cceg.ki.se/documents/ChildhoodCancerIncidenceandSurvivalinSweden1984_2010. pdf.
4. McGregor LM, Metzger ML, Sanders R, Santana VM. Pediatric cancers in the new millennium: dramatic progress, new challenges. *Oncology* 2007; **21**: 809–820; discussion 820, 823–804.
5. Armstrong GT, Liu Q, Yasui Y, Huang S, Ness KK, Leisenring W *et al.* Long-term outcomes among adult survivors of childhood central nervous system malignancies in the Childhood Cancer Survivor Study. *J Natl Cancer Inst* 2009; **101**: 946–958.
6. Lannering B, Marky I, Lundberg A, Olsson E. Long-term sequelae after pediatric brain tumors: their effect on disability and quality of life. *Med Pediatr Oncol* 1990; **18**: 304–310.
7. Lahteenmaki PM, Harila-Saari A, Pukkala EI, Kyyronen P, Salmi TT, Sankila R. Scholastic achievements of children with brain tumors at the end of comprehensive education: a nationwide, register-based study. *Neurology* 2007; **69**: 296–305.
8. Ris MD, Packer R, Goldwein J, Jones-Wallace D, Boyett JM. Intellectual outcome after reduced-dose radiation therapy plus adjuvant chemotherapy for medulloblastoma: a Children's Cancer Group study. *J Clin Oncol* 2001; **19**: 3470–3476.
9. Fouladi M, Gilger E, Kocak M, Wallace D, Buchanan G, Reeves C *et al.* Intellectual and functional outcome of children 3 years old or younger who have CNS malignancies. *J Clin Oncol* 2005; **23**: 7152–7160.
10. Reddick WE, Russell JM, Glass JO, Xiong X, Mulhern RK, Langston JW *et al.* Subtle white matter volume differences in children treated for medulloblastoma with conventional or reduced dose craniospinal irradiation. *Magn Reson Imaging* 2000; **18**: 787–793.
11. Calvo W, Hopewell JW, Reinhold HS, Yeung TK. Time- and dose-related changes in the white matter of the rat brain after single doses of X rays. *Br J Radiol* 1988; **61**: 1043–1052.
12. Oi S, Kokunai T, Ijichi A, Matsumoto S, Raimondi AJ. Radiation-induced brain damage in children–histological analysis of sequential tissue changes in 34 autopsy cases. *Neurologia Medico-Chirurgica* 1990; **30**: 36–42.
13. Kuhn HG, Blomgren K. Developmental dysregulation of adult neurogenesis. *Eur J Neurosci* 2011; **33**: 1115–1122.
14. Raber J, Rola R, LeFevour A, Morhardt D, Curley J, Mizumatsu S *et al.* Radiation-induced cognitive impairments are associated with changes in indicators of hippocampal neurogenesis. *Radiat Res* 2004; **162**: 39–47.
15. Altman J. Morphological and behavioral markers of environmentally induced retardation of brain development: an animal model. *Environ Health Perspect* 1987; **74**: 153–168.
16. Mulhern RK, Palmer SL, Reddick WE, Glass JO, Kun LE, Taylor J *et al.* Risks of young age for selected neurocognitive deficits in medulloblastoma are associated with white matter loss. *J Clin Oncol* 2001; **19**: 472–479.
17. Reddick WE, Glass JO, Palmer SL, Wu S, Gajjar A, Langston JW *et al.* A typical white matter volume development in children following craniospinal irradiation. *Neuro Oncol* 2005; **7**: 12–19.
18. Palmer SL, Reddick WE, Glass JO, Gajjar A, Goloubeva O, Mulhern RK. Decline in corpus callosum volume among pediatric patients with medulloblastoma: longitudinal MR imaging study. *AJNR Am J Neuroradiol* 2002; **23**: 1088–1094.
19. Luders E, Thompson PM, Toga AW. The development of the corpus callosum in the healthy human brain. *J Neurosci* 2010; **30**: 10985–10990.
20. Lenroot RK, Gogtay N, Greenstein DK, Wells EM, Wallace GL, Clasen LS *et al.* Sexual dimorphism of brain developmental trajectories during childhood and adolescence. *Neuroimage* 2007; **36**: 1065–1073.
21. Lenroot RK, Giedd JN. Brain development in children and adolescents: insights from anatomical magnetic resonance imaging. *Neurosci Biobehav Rev* 2006; **30**: 718–729.
22. Fukuda A, Fukuda H, Jonsson M, Swanpalmer J, Hertzman S, Lannering B *et al.* Progenitor cell injury after irradiation to the developing brain can be modulated by mild hypothermia or hyperthermia. *J Neurochem* 2005; **94**: 1604–1619.
23. Goldberg JS, Hirschi KK. Diverse roles of the vasculature within the neural stem cell niche. *Regen Med* 2009; **4**: 879–897.
24. Pham LD, Hayakawa K, Seo JH, Nguyen MN, Som AT, Lee BJ *et al.* Crosstalk between oligodendrocytes and cerebral endothelium contributes to vascular remodeling after white matter injury. *Glia* 2012; **60**: 875–881.
25. Bostrom M, Kalm M, Karlsson N, Hellstrom Erkenstam N, Blomgren K. Irradiation to the young mouse brain caused long-term, progressive depletion of neurogenesis but did not disrupt the neurovascular niche. *J Cereb Blood Flow Metab* 2013; **33**: 935–943.
26. Wakisaka S, O'Neill RR, Kemper TL, Verrelli DM, Caveness WF. Delayed brain damage in adult monkeys from radiation in the therapeutic range. *Radiat Res* 1979; **80**: 277–291.
27. Roughton K, Kalm M, Blomgren K. Sex-dependent differences in behavior and hippocampal neurogenesis after irradiation to the young mouse brain. *Eur J Neurosci* 2012; **36**: 2763–2772.
28. Villasana L, Rosenberg J, Raber J. Sex-dependent effects of 56Fe irradiation on contextual fear conditioning in C57BL/6J mice. *Hippocampus* 2010; **20**: 19–23.
29. Hellstrom NA, Bjork-Eriksson T, Blomgren K, Kuhn HG. Differential recovery of neural stem cells in the subventricular zone and dentate gyrus after ionizing radiation. *Stem Cells* 2009; **27**: 634–641.
30. Fukuda H, Fukuda A, Zhu C, Korhonen L, Swanpalmer J, Hertzman S *et al.* Irradiation-induced progenitor cell death in the developing brain is resistant to erythropoietin treatment and caspase inhibition. *Cell Death Differ* 2004; **11**: 1166–1178.
31. Fukuda A, Fukuda H, Swanpalmer J, Hertzman S, Lannering B, Marky I *et al.* Age-dependent sensitivity of the developing brain to irradiation is correlated with the number and vulnerability of progenitor cells. *J Neurochem* 2005; **92**: 569–584.
32. Akiyama K, Tanaka R, Sato M, Takeda N. Cognitive dysfunction and histological findings in adult rats one year after whole brain irradiation. *Neurologia Medico-Chirurgica* 2001; **41**: 590–598.
33. Christie D, Leiper AD, Chessells JM, Vargha-Khadem F. Intellectual performance after presymptomatic cranial radiotherapy for leukaemia: effects of age and sex. *Arch Dis Child* 1995; **73**: 136–140.
34. Mulhern RK, Merchant TE, Gajjar A, Reddick WE, Kun LE. Late neurocognitive sequelae in survivors of brain tumours in childhood. *Lancet Oncol* 2004; **5**: 399–408.
35. Palmer SL, Glass JO, Li Y, Ogg R, Qaddoumi I, Armstrong GT *et al.* White matter integrity is associated with cognitive processing in patients treated for a posterior fossa brain tumor. *Neuro Oncol* 2012; **14**: 1185–1193.
36. Semple BD, Blomgren K, Gimlin K, Ferriero DM, Noble-Haeusslein LJ. Brain development in rodents and humans: Identifying benchmarks of maturation and vulnerability to injury across species. *Prog Neurobiol* 2013; **106-107**: 1–16.
37. Crow TJ, Paez P, Chance SA. Callosal misconnectivity and the sex difference in psychosis. *Int Rev Psychiatry (Abingdon, England)* 2007; **19**: 449–457.
38. Mark F, Bear BWC, Michael AP. *Neuroscience, Exploring the Brain*. 3rd edn, Lippincott Williams & Wilkins, 2007.
39. Krinke GJ. *The Laboratory Rat*. Academic: San Diego, CA, USA, 2000.
40. Skoff RP, Knapp PE. Division of astroblasts and oligodendroblasts in postnatal rodent brain: evidence for separate astrocyte and oligodendrocyte lineages. *Glia* 1991; **4**: 165–174.
41. Panagiotakos G, Alshamy G, Chan B, Abrams R, Greenberg E, Saxena A *et al.* Long-term impact of radiation on the stem cell and oligodendrocyte precursors in the brain. *PLoS One* 2007; **2**: e588.
42. Bellinzona M, Gobbel GT, Shinohara C, Fike JR. Apoptosis is induced in the subependyma of young adult rats by ionizing irradiation. *Neurosci Lett* 1996; **208**: 163–166.
43. Kurita H, Kawahara N, Asai A, Ueki K, Shin M, Kirino T. Radiation-induced apoptosis of oligodendrocytes in the adult rat brain. *Neurol Res* 2001; **23**: 869–874.
44. Bradl M, Lassmann H. Oligodendrocytes: biology and pathology. *Acta neuropathologica* 2010; **119**: 37–53.
45. Limoli CL, Giedzinski E, Rola R, Otsuka S, Palmer TD, Fike JR. Radiation response of neural precursor cells: linking cellular sensitivity to cell cycle checkpoints, apoptosis and oxidative stress. *Radiat Res* 2004; **161**: 17–27.
46. Manda K, Ueno M, Anzai K. Memory impairment, oxidative damage and apoptosis induced by space radiation: ameliorative potential of alpha-lipoic acid. *Behav Brain Res* 2008; **187**: 387–395.
47. Spitz DR, Azzam EI, Li JJ, Gius D. Metabolic oxidation/reduction reactions and cellular responses to ionizing radiation: a unifying concept in stress response biology. *Cancer Metastasis Rev* 2004; **23**: 311–322.
48. Chari DM, Huang WL, Blakemore WF. Dysfunctional oligodendrocyte progenitor cell (OPC) populations may inhibit repopulation of OPC depleted tissue. *J Neurosci Res* 2003; **73**: 787–793.
49. Cerghet M, Skoff RP, Swamydas M, Bessert D. Sexual dimorphism in the white matter of rodents. *J Neurol Sci* 2009; **286**: 76–80.
50. Karlsson N, Kalm M, Nilsson MK, Mallard C, Bjork-Eriksson T, Blomgren K. Learning and activity after irradiation of the young mouse brain analyzed in adulthood using unbiased monitoring in a home cage environment. *Radiation Res* 2011; **175**: 336–346.
51. Ohab JJ, Fleming S, Blesch A, Carmichael ST. A neurovascular niche for neurogenesis after stroke. *J Neurosci* 2006; **26**: 13007–13016.
52. McDonald LW, Hayes TL. The role of capillaries in the pathogenesis of delayed radionecrosis of brain. *Am J Pathol* 1967; **50**: 745–764.
53. Reinhold HS, Calvo W, Hopewell JW, van der Berg AP. Development of blood vessel-related radiation damage in the fimbria of the central nervous system. *Int J Radiat Oncol Biol Phys* 1990; **18**: 37–42.
54. Fowler JF. The linear-quadratic formula and progress in fractionated radiotherapy. *Br J Radiol* 1989; **62**: 679–694.
55. Zhu C, Gao J, Karlsson N, Li Q, Zhang Y, Huang Z *et al.* Isoflurane anesthesia induced persistent, progressive memory impairment, caused a loss of neural stem cells, and reduced neurogenesis in young, but not adult, rodents. *J Cereb Blood Flow Metab* 2010; **30**: 1017–1030.
56. Kalm M, Lannering B, Bjork-Eriksson T, Blomgren K. Irradiation-induced loss of microglia in the young brain. *J Neuroimmunol* 2009; **206**: 70–75.
57. Persson A, Osman A, Mallard C, Bolouri H, Kuhn HG. Radixin expression in microglia after cortical stroke lesion. *Glia* 2013; **61**: 790–799.
58. Kalm M, Fukuda A, Fukuda H, Ohrfelt A, Lannering B, Bjork-Eriksson T *et al.* Transient inflammation in neurogenic regions after irradiation of the developing brain. *Radiat Res* 2009; **171**: 66–76.

59. Jarlestedt K, Rousset CI, Faiz M, Wilhelmsson U, Stahlberg A, Sourkova H *et al*. Attenuation of reactive gliosis does not affect infarct volume in neonatal hypoxic-ischemic brain injury in mice. *PLoS One* 2010; **5**: e10397.
60. Zhu C, Wang X, Hagberg H, Blomgren K. Correlation between caspase-3 activation and three different markers of DNA damage in neonatal cerebral hypoxia-ischemia. *J Neurochem* 2000; **75**: 819–829.